Available online at www.sciencedirect.com

SCIENCE DIRECT®

Journal of Molecular Catalysis A: Chemical 204–205 (2003) 637–646

JOURNAL OF MOLECULAR CATALYSIS A: CHEMICAL

www.elsevier.com/locate/molcata

Ni based mixed oxide materials for CH_4 oxidation under redox cycle conditions

Raffaella Villa [a], Cinzia Cristiani [a], Gianpiero Groppi [a], Luca Lietti [a,*], Pio Forzatti [a], Ugo Cornaro [b], Stefano Rossini [b]

[a] *CMIC, Dipartimento di Chimica, Materiali e Ingegneria Chimica, "Giulio Natta", Politecnico di Milano, Piazza Leonardo da Vinci 32, I-20133 Milan, Italy*

[b] *Snamprogetti, Via Maritano, S. Donato Milanese, Milan, Italy*

Received 21 October 2002; received in revised form 17 February 2003; accepted 5 March 2003

Dedicated to Professor Renato Ugo on the occasion of his 65th birthday

Abstract

The preparation, characterization and redox properties of Ni–Al–O and Ni–Mg–Al–O mixed oxides for CH_4 chemical looping combustion (CLC) is addressed in this study. Ni–Al–O samples having different Ni/Al ratios (0.5–2.25), prepared by coprecipitation, consist after calcination at 1000 °C of cubic NiO and $NiAl_2O_4$ spinel. A similar phase composition is obtained for Ni–Mg–Al–O, with Mg partitioned in the two phases. The presence of $NiAl_2O_4$ prevents the crystal size growth of NiO with respect to pure NiO; further limit of the sintering of the cubic oxide was observed in presence of Mg. Reduction of the samples by H_2 occurs in two steps, associated with reduction of Ni^{2+} in NiO and $NiAl_2O_4$. Mg stabilizes Ni^{2+} in both the cubic oxide and the spinel phase and improves regenerability upon repeated redox cycles. Temperature programmed reduction with CH_4 (CH_4-TPR) experiments showed poor selectivity to CO_2 and H_2O, being CO and H_2 the most abundant products. Also, formation of coke is observed over the samples. The same behavior is observed in CH_4/O_2 pulse experiments; however, in the case of the Mg-containing system, coke formation can be avoided by co-feeding H_2O along with CH_4.

Keywords: Ni based catalysts; Redox materials; Methane oxidation; Chemical looping combustion; Mg-doping

1. Introduction

Chemical looping combustion (CLC) has been proposed as an energy conversion process with good potential to provide CO_2 capture with low cost while keeping high energy efficiency [1–3]. In such a process combustion is carried out in two separate reactors: in the first one (oxidizer) the fuel is oxidized using a reducible metal oxide as oxygen carrier, while in the second reactor (regenerator) the reduced material, generated in the first step, is re-oxidized by air. The redox material is continuously re-circulated between the two reactors. The hot air stream from the regenerator is expanded in a gas turbine for production of energy, whereas the stream from the oxidizer, consisting of CO_2 and H_2O, is sent to a CO_2 separation unit where the high CO_2 concentration allows for its economical recovery.

* Corresponding author. Tel.: +39-02-2399-3272; fax: +39-02-7063-8173.
E-mail address: luca.lietti@polimi.it (L. Lietti).

1381-1169/$ – see front matter © 2003 Elsevier Science B.V. All rights reserved.
doi:10.1016/S1381-1169(03)00346-7

The development of the CLC process relies on the availability of redox materials able to match the following requirements: (i) good redox reactivity with high selectivity towards complete oxidation products; (ii) high oxygen exchange efficiency, i.e. ratio of the oxygen mass involved in the redox process to the total mass of the solid; (iii) regenerability, i.e. stability during repeated redox cycles at relatively high temperature (above 800 °C); (iv) mechanical resistance to the friction stresses associated with recirculation of solid powders; (v) low cost.

On the basis of thermodynamic considerations [4,5] materials based on Ni, Co or Fe were identified as potential candidates for CLC. Among these, Ni oxides show the following promising features: (i) negligible volatility of Ni species below 1000 °C [6]; (ii) well assessed high temperature applications such as steam reforming and secondary reforming [7].

Ishida and Jin [3] and Ishida and co-workers [8] investigated the redox properties of NiO, pure and dispersed with different inorganic binders including MgO, Y-stabilized ZrO_2 (YSZ) and $NiAl_2O_4$ by means of thermogravimetric measurements during redox cycles at constant temperature and of chemical looping combustion with solid recirculation [9]. They observed that upon reduction in H_2 at 600 °C pure NiO cannot be completely re-oxidized in air at 1000 °C whereas reoxidation rapidly occurs when NiO particles are thoroughly mixed either with an YSZ or with a $NiAl_2O_4$ binder. A NiO/$NiAl_2O_4$ (weight ratio 60/40) system prepared via dissolution/precipitation methods was reported as the best performing material in terms of regenerability upon several redox cycles using both H_2 and CH_4 as reductants.

In this paper the redox properties of Ni–Al–O systems prepared via co-precipitation in aqueous medium with Ni/Al varying between 0.5 and 2.25 were systematically investigated along with those of a Ni–Mg–Al–O system with atomic ratios Ni/Mg = 1/1 and (Ni + Mg)/Al = 1. The redox performances were screened by means of repeated temperature programmed reduction (TPR)/ temperature programmed oxidation (TPO) cycles. Pulse experiments with CH_4 were also performed on selected systems to evaluate the products distribution of CH_4 oxidation.

2. Experimental

2.1. Preparation

Samples having nominal composition $(NiO)_x$/$NiAl_2O_4$ (with $x = 0$, 0.4, 1.0, 3.5, corresponding to Ni/Al atomic ratio of 0.5, 0.7, 1 and 2.25, respectively) and Mg-containing sample having (Ni + Mg)/Al and Ni/Mg ratios both equal to 1.0 were prepared by co-precipitation in aqueous medium. Weighted amounts of Ni, Al and Mg nitrates were dissolved in water at about 60 °C to obtain a solution with a final concentration $[M^{2+} + M^{3+}] \cong 1$ M. An $(NH_4)_2CO_3$ solution was used as precipitating agent (final concentration $\cong$ 2 M). Excess of $(NH_4)_2CO_3$ (60–70%) was used with respect to the stoichiometric ratio $(NH_4)_2CO_3/M^{n+} = n/2$ mol/mol ($M^{n+} = Ni^{2+}$, Mg^{2+} and Al^{3+}), as indicated by preliminary potentiometric titration curves. Precipitation was achieved by rapidly pouring the nitrate solution into the carbonate one. The slurry was aged for 3 h at 60 °C; during precipitation and aging the pH remained constant in the range 6.5–7. The effectiveness of the precipitation route for Ni/Al catalyst samples was confirmed by analysis of the mother liquors, which showed negligible weight losses for Ni and Al, indicating that precipitation was quantitative. On the other hand in the case of the Mg-containing sample a Mg loss of about 12% of the nominal value was determined, possibly associated with the relatively low value of pH used during precipitation.

After aging the solid was filtered, washed, dried at 110 °C overnight and finally calcined at 1000 °C for 10 h (heating/cooling at 1 °C/min).

2.2. Characterization

X-ray diffraction (XRD) analyses were performed on the powder materials by a Philips goniomether (PW 1050/70) using a Ni-filtered Cu Kα radiation (λ = 1.542 Å). XRD data were refined by Rietveld analysis using the GSAS software package by Larson and Von Dreele [10]. Crystallite dimensions were calculated with the Sherrer equation [11] using the Lorentian part of the full-width at half-maximum (FWHM) obtained by Rietveld analysis.

Temperature programmed reduction with H_2 (H_2-TPR)–TPO was performed with a ThermoQuest

TPDRO 1100 apparatus with H_2/Ar (H_2 = 5% (v/v)) and O_2/He (O_2 = 2% (v/v)) mixtures, respectively (flow rate 30 Ncc/min, heating rate: 7 °C/min). Hundred milligrams of calcined sample were used in the experiments; the sequence involved a series of TPR/TPO runs with an inert purge in between. TPR/TPO cycles were also performed with CH_4 (1.6% (v/v) in He) as reducing agent temperature programmed reduction with CH_4 (CH_4-TPR). In this case a dedicated apparatus equipped with a quadrupole mass spectrometer was used, which allowed detection of the various reaction products. 120 mg of calcined sample was used in each experiment, and a heating schedule of 15 °C/min was adopted. Further details on the experimental apparatus can be found elsewhere [12].

2.3. Activity runs

The catalyst activity under reducing–oxidising conditions at constant temperature was also investigated by flowing alternatively two gas blends (CH_4 50% (v/v) in He and O_2 20% (v/v) in He) through the catalyst with Ar purge in between, while continuously analyzing the reaction products by on-line mass spectrometry (pulse experiments). The different flows were supplied by two automated four-way switching valves. Experimental conditions were as follows: catalyst weight 2 g, gas flow rate 20 cm^3/min @STP, T = 800 °C. Runs were also performed in the presence of water vapor in the feed during the CH_4 switch ($CH_4/H_2O = 1/1$).

$(NiO)_x/NiAl_2O_4$ samples will be identified in the text according to their Ni/Al ratio and treatment type (D: dried; C: calcined; R: reduced in H_2) and temperature: e.g. Ni/Al-2.25-C600 identifies the sample with nominal Ni/Al ratio of 2.25 (i.e. 60% (w/w) NiO–40% (w/w) $NiAl_2O_4$), calcined at 600 °C. The Mg-containing sample will be denoted as NiMgAl.

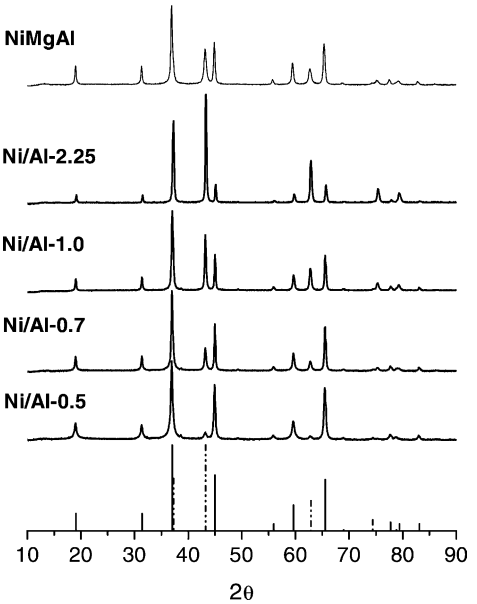

Fig. 1. XRD spectra of the samples calcined at 1000 °C. Solid line: spinel phase; dashed lines: cubic oxide phase.

3. Results and discussion

3.1. Catalyst characterization

The XRD spectra of the samples calcined at 1000 °C are shown in Fig. 1. The reflections of well crystallized NiO (o) [JCPDS 47-1049] and $NiAl_2O_4$ (s) [JCPDS 10-339] are well evident. XRD spectra have been analyzed by Rietveld analysis that allows for both quantitative analysis and calculation of crystallite dimensions of the present phases. The results are reported in Table 1 as a function of the Ni/Al ratio. Data obtained from pure NiO sample prepared according to a similar precipitation procedure are also reported for comparison.

Table 1
Quantitative and crystallite dimension, calculated by Rietveld analysis, of NiO and $NiAl_2O_4$ in the samples calcined at 1000 °C

Sample	NiO expected (%)	NiO calculated (%)	NiO d_{cr} (nm)	$NiAl_2O_4$ expected (%)	$NiAl_2O_4$ calculated (%)
NiO	100	100	150	–	–
Ni/Al-0.5	0	6	13	100	94
Ni/Al-0.7	15	19	11.5	85	81
Ni/Al-1.0	30	38	34	70	62
Ni/Al-2.25	60	67	44	40	33

To address the sintering behavior of NiO, which could be relevant to the redox properties herein investigated, its crystal size was determined. The calculated values are reported in Table 1 as a function of Ni/Al ratio; data obtained from pure NiO sample prepared according to a similar precipitation procedure are also reported for comparison. An effect of the Ni/Al ratio on NiO sintering is evident, since its crystal size increases on increasing the excess of Ni with respect to the stoichiometric spinel composition. It is worth noting that pure NiO sample markedly sinters to a crystal size >100 nm upon calcination at 1000 °C. This suggests that intimate mixing between $NiAl_2O_4$ and NiO obtained via co-precipitation has a marked dispersion effect on NiO; this effect decreases on increasing the $NiO/NiAl_2O_4$ ratio. In the case of $NiAl_2O_4$ crystallite dimensions in the range 30–40 nm were calculated.

Rietveld analysis also allowed calculation of the amounts of the two phases. A small excess of NiO (5–8% (w/w)) is systematically calculated with respect to the expected values. Such a discrepancy may be due to the formation of a substoichiometric spinel phase: in fact, according to the Ni–Al–O phase diagram [13], the spinel $NiAl_2O_4$ phase is stable for Ni/Al ratios in the range 0.35–0.5.

Upon calcination at 1000 °C the characteristic reflection of a mixed cubic oxide and of a spinel phase are also present in the Mg-containing sample (Fig. 1). Compositions of the two phases were estimated according to the Viggard's law, by comparing the cell parameters calculated by Rietveld analysis (cubic oxide: $a_0 = 4.1879(5)$ Å; spinel type phase: $a_0 = 8.0720(7)$ Å) with those reported in the literature for MgO ($a_0 = 4.211$ Å [JCPDS 45-946]) and NiO ($a_0 = 4.177$ Å), and for $NiAl_2O_4$ ($a_0 = 8.04800$ Å) and $MgAl_2O_4$ ($a_0 = 8.0831$ Å [JCPDS 21-1152]), respectively. The following degree of Mg substitution was determined: $x = 0.36$ in $Ni_{1-x}Mg_xO$ and $y = 0.69$ in $Ni_{1-y}Mg_yAl_2O_4$. Calculated crystal size of the $Ni_{0.64}Mg_{0.36}O$ ($d_{cr} = 17$ nm) in the sample calcined at 1000 °C evidences a dispersion effect of the spinel matrix even more efficient than that observed for the Ni/Al-1.0-C1000 sample ($d_{cr} = 34$ nm). Also in this sample crystallite dimensions of the spinel phase were about 30 nm.

3.2. Redox properties

The redox characteristics of the samples were investigated by TPR/TPO experiments with H_2 or CH_4 as reducing agents. The use of H_2 allowed us to compare the present results with literature data; on the other hand the use of methane is of interest being the reductant in the CLC process.

Fig. 2 shows the results of the H_2-TPR analysis performed over the Ni/Al samples calcined at 1000 °C. The TPR profile recorded in the case of the Mg-containing sample is also reported.

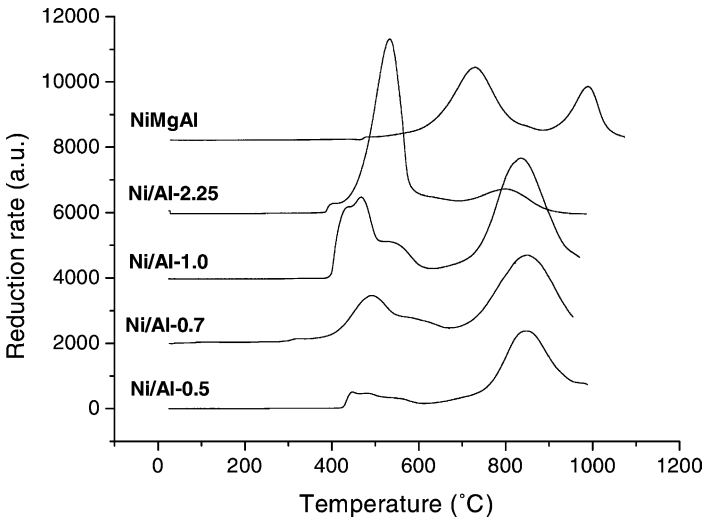

Fig. 2. H_2-TPR of the samples calcined at 1000 °C.

In the case of the Ni/Al samples the TPR spectra show a complex profile, with a low H_2 consumption peak centered in the 400–600 °C temperature range and a high temperature peak with maximum near 850 °C. In line with literature data [14,15] the peak in the temperature range 400–600 °C is attributed to the reduction of Ni^{2+} in the NiO phase, its complexity may be ascribed to the presence of different NiO species [15]. On the other hand, the well defined high temperature TPR peak at 850 °C is associated with the reduction of Ni^{2+} in $NiAl_2O_4$. TPR profiles are consistent with XRD data previously shown which indicated the presence in the samples of both NiO and $NiAl_2O_4$ phases after calcination at 1000 °C. As a matter of facts, on increasing the Ni/Al ratio an increase of the relative abundance of the low temperature TPR peak is observed, in line with the increased $NiO/NiAl_2O_4$ ratio pointed out by XRD.

In the case of the NiMgAl sample, two TPR peaks are also evident, centered at 720 and 1000 °C, respectively. These peaks can be reasonably associated with the reduction of Ni^{2+} in the mixed $Ni_{1-x}Mg_xO$ and $Ni_{1-y}Mg_yAl_2O_4$ phases, respectively. A comparison with the TPR profiles obtained in the case of the Mg-free samples shows that the presence of Mg shifts towards higher temperatures the reduction temperatures of Ni^{2+} species with respect to both the pure NiO and $NiAl_2O_4$ phases. Accordingly a temperature of 1100 °C is required to achieve complete reduction of the Mg-containing sample. The shift towards higher temperatures of the Ni^{2+} reduction peak in NiO in the presence of Mg is well documented in the literature [16], and was associated to the formation of a NiO–MgO solid solution in which Ni^{2+} ions are stabilized against reduction and sintering by the MgO-type matrix. A similar effect may also be invoked for explaining the temperature shift observed for Ni^{2+} in $Ni_{1-y}Mg_yAl_2O_4$ as compared to $NiAl_2O_4$.

After H_2-TPR, the catalyst samples were cooled at RT under Ar flow and reoxidized with O_2/He up to 1000 °C (TPO). Three to four TPR/TPO cycles were sequentially performed on each catalyst sample, aiming at investigating the reversibility of the reduction–oxidation processes. In these experiments a maximum reduction temperature of 1000 and 1100 °C were adopted for the Ni/Al and NiMgAl systems, respectively, in order to complete reduction of all the Ni species. In the case of the Ni/Al samples, the results of TPO experiments (herein not shown for brevity) showed that reoxidation of the reduced samples occurs in the 200–600 °C temperature range with a complex feature involving partially overlapping steps possibly associated with the reoxidation of the different Ni species. A similar behavior is apparent for the Mg-containing sample (NiMgAl) as well; only a slight decrease of the temperature onset for catalyst reoxidation was observed.

The sequence of TPR/TPO cycles performed on the Ni/Al systems pointed out a progressive decrease of both the TPR and TPO signals, suggesting that the Ni/Al samples are not stable under repeated reduction–oxidation cycles. This is consistent with recent report from Ishida et al. [9] showing modification of the redox behavior of a 60/40 (w/w) $NiO/NiAl_2O_4$ system upon ten isothermal redox cycles at 900 °C. On the other hand, in the case of the NiMgAl sample, the TPR/TPO profiles were practically superimposed in each cycle. This clearly indicates that the presence of Mg, besides modifying the catalyst reducibility (see above), greatly increases the stability of Ni/Al catalysts under repeated reduction–oxidation cycles.

XRD spectra performed over the samples discharged after the last TPO run revealed, in the case of the Ni/Al systems, the presence of a well crystallized metallic Ni phase (30–50 nm), along with NiO and $NiAl_2O_4$. The amount of the metallic Ni phase increases with the Ni/Al ratio. On the other hand, XRD spectra showed that no metallic Ni was formed on discharged NiMgAl, which indeed does not show any phase modification with respect to the calcined sample.

In order to check the possibility that irreversibility in the reduction process may be ascribed to the reduction of the $NiAl_2O_4$ phase, TPR/TPO cycles were performed with $T_{max} = 700$ °C (900 °C for the NiMgAl sample), i.e. before the temperature onset for Ni^{2+} reduction in the spinel phase. The results, shown in Fig. 3A and B for the Ni/Al-1.0 and NiMgAl samples, respectively, indicated that even below 700 °C the Ni/Al samples exhibited a non-reversible redox behavior. As a matter of facts, also in this case XRD analysis performed on the discharged sample showed the presence of small amounts (5%) of metallic Ni. On the other hand, in line with previous data, the NiMgAl sample showed a reversible redox behavior following several TPR/TPO runs. XRD analysis

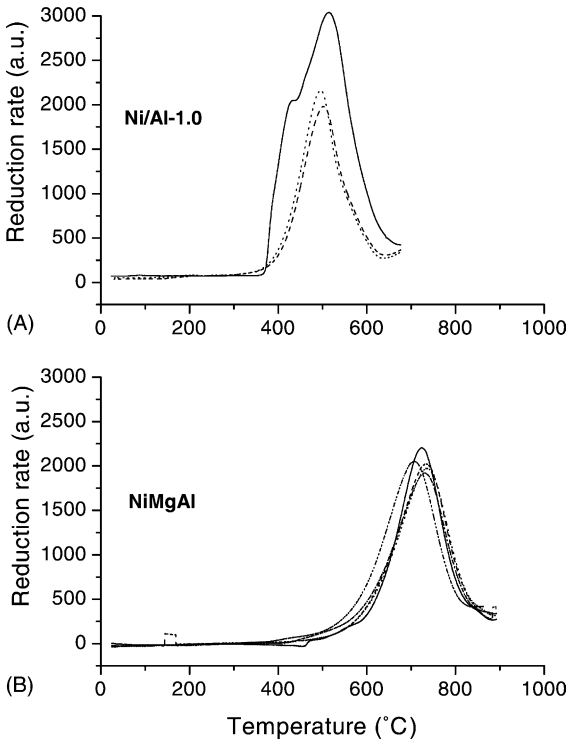

Fig. 3. Repeated H_2-TPR cycles performed over Ni/Al-1.0 (A) and NiMgAl (B) samples. Reoxidation was performed at 1000 °C. Solid lines: run 1; dashed lines: run 2; dotted lines: run 3; dash–dot lines: run 4; dash–dot–dot lines: run 5.

of the discharged sample did not showed any significant phase and crystal size variation neither in the Ni–Mg–O phase nor in the spinel phase.

The catalyst redox properties were also investigated by alternating CH_4-TPR/TPO runs. Aim of these experiments was to provide information on the selectivity of the reducing process, which was not previously addressed in the literature [8], as well as on the reversibility of the catalyst redox properties under reducing atmosphere relevant to the process under study. Only two samples out of the prepared systems were tested in these conditions, i.e. Ni/Al-2.25 and NiMgAl. In the case of Ni/Al-2.25 (data not reported), methane is converted starting from 550 °C, i.e. well above the temperature threshold for H_2 consumption in H_2-TPR experiments (see Fig. 2). This is in line with the poor reducing capability of CH_4 if compared with H_2. CH_4 oxidation is poorly selective towards the formation of total oxidation products (CO_2 and H_2O), since relevant amounts of CO and H_2 are formed. Furthermore, carbonaceous deposits are also formed on the catalyst surface, as pointed out by the formation of CO and CO_2 during the subsequent reoxidation (TPO). Besides, upon repeated TPR/TPO cycles the catalyst redox behavior was not found fully reversible.

The results of CH_4-TPR/TPO cycles performed on the NiMgAl catalyst sample are reported in Fig. 4A and B, respectively. As shown in the figure, CH_4 is rapidly consumed near 570 °C; again a comparison with previous H_2/TPR data shows the lower reactivity of CH_4 if compared to H_2. The methane concentration profile shows a complex behavior with minima at 750 and 1000 °C, this latter corresponding to the end of the TPR run. Notably, the reduction process is fully selective towards the formation of H_2/CO. The evolution with temperature of CO/H_2 is rather complex: this is likely related to the simultaneous occurrence of several reactions involving different active sites, i.e. oxidized Ni species (lattice oxygen) and reduced Ni formed upon reduction of Ni^{2+}. The formation of small amounts of CO_2 and H_2O via reaction of CH_4 with lattice oxygen species cannot be excluded; however they are completely consumed via consecutive CH_4 reforming reactions leading to CO and H_2 on reduced Ni sites, which are well known reforming catalyst [17]. An excess of H_2 with respect to CO is observed in the range 800–900 °C, which can be ascribed to the decomposition of CH_4 leading to deposition of carbon.

In the subsequent TPO run (Fig. 4B), the catalyst is reoxidized starting from 200 °C, i.e. in well agreement with previous TPO runs following H_2-TPR experiments. O_2 concentration shows a minimum near 550 °C. Catalyst reoxidation is accompanied by the formation of CO and CO_2, due to the oxidation of carbon deposits formed during the previous CH_4-TPR run.

Repeated TPR/TPO cycles performed over MgNiAl showed a few differences in the concentration profiles of the various species versus temperature; however complete selectivity towards CO/H_2 was always observed during the CH_4-TPR runs. Such a lack of reversibility, which contrasts previous H_2-TPR data, may be ascribed to the presence of carbonaceous deposits formed during the reaction of methane.

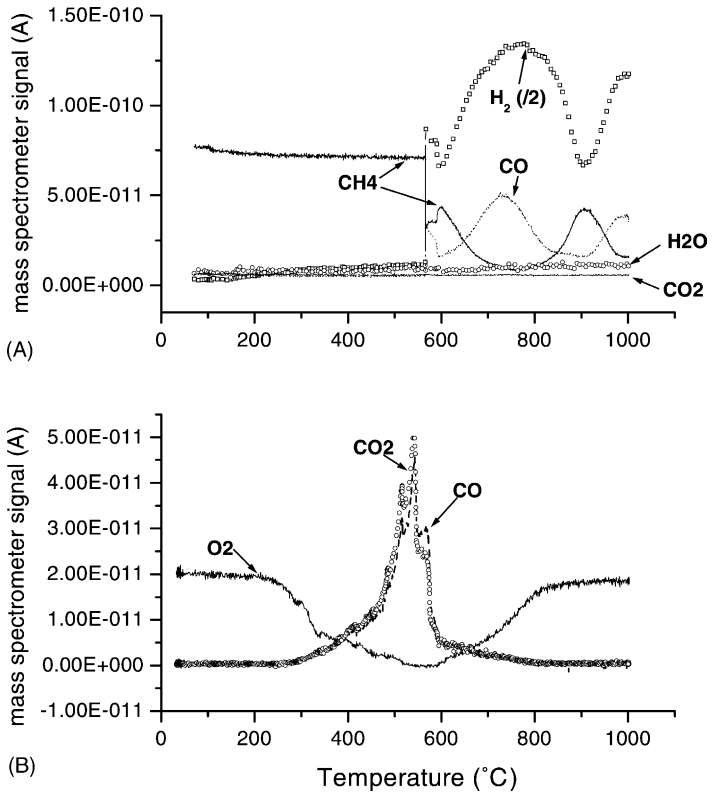

Fig. 4. (A and B) CH_4-TPR/TPO experiments performed on NiMgAl (mass spectrometer signals vertically shifted for clarity).

3.3. Catalyst activity under alternating reducing–oxidising conditions (pulse experiments)

Finally, the reactivity of the NiMgAl sample was also investigated at constant temperature (800 °C) by alternating reducing–oxidising conditions. Aim of these experiments was to analyze the sample reactivity at constant temperature as a function of the catalyst degree of reduction. Experiments were performed in the absence and in the presence of water during the CH_4 switch, and results are reported in Fig. 5A and B, respectively, as product concentration profiles versus time on stream. In the case of the dry feed (Fig. 5A), upon admission of CH_4 to the reactor (reduction step), CO, CO_2, H_2 and H_2O are formed. No CH_4 was observed during the whole duration of the switch (200 s), thus indicating that methane conversion was complete. It is noted that the duration of the CH_4 switch was kept short in order to avoid reactor plugging due to the formation of carbonaceous deposits. The concentration profiles of the various reaction products show different dynamics: indeed while CO_2 and H_2O (with a small delay) appear as a sharp peak immediately after CH_4 admission, CO and H_2 show a slower increase during the pulse. The change in the product selectivity during the reduction step can be likely associated to changes in the catalyst degree of oxidation. It may be speculated that at the beginning of the CH_4 switch the fully oxidized catalyst favors the total oxidation of methane, although total selectivity to deep oxidation products is not achieved. As the sample is being reduced, the product formation switches from CO_2 and H_2O to more CO and H_2, possibly assisted by the occurrence of methane reforming reactions (steam and dry) involving water and CO_2 and catalyzed by reduced Ni sites. The weak maximum in the CO_2 concentration which is observed immediately after the switch to inert gas atmosphere is likely due to the desorption of CO_2 from the catalyst surface.

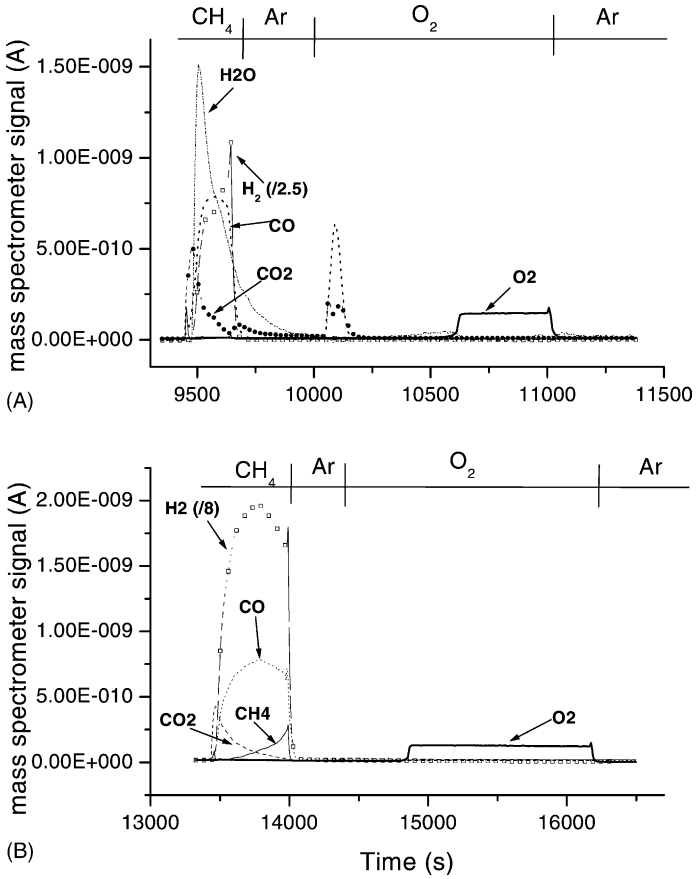

Fig. 5. Pulse experiments performed at 800 °C on NiMgAl. (A) CH_4 dry feed; (B) CH_4 wet feed ($CH_4/H_2O = 1$).

These results appear at variance of CH_4-TPR data previously reported; indeed in that case neither CO_2 nor water were formed, and selectivity was complete to H_2 and CO. One can speculate that in the case of the CH_4-TPR run, where CH_4 reactivity is monitored at lower temperatures (starting from 570 to 800 °C), the reactivity of lattice oxygen species is different and this would favor the formation of CH_4 partial oxidation products instead of CO_2 and H_2O. However, as reported above, it cannot be excluded that during TPR runs minor amounts of carbon dioxide and water are also formed, which are readily consumed in consecutive CH_4 reforming reactions.

Following the CH_4 switch, the catalyst is reoxidized by air. Upon O_2 admission to the reactor, CO and CO_2 immediately appear at the reactor outlet. The formation of such species is related to the oxidation of carbonaceous deposits accumulated in the previous reducing switch. Catalyst reoxidation is completed well after the complete oxidation of carbon deposits, as indicated by the delay that is observed between the CO and CO_2 evolution and the O_2 breakthrough.

Pulse experiments were also performed in the presence of water vapor during the CH_4 switch, and results are reported in Fig. 5B. In this case it was possible to increase the duration of the CH_4 switch due to the presence of water which limited the formation of carbonaceous deposits. In any case, the length of the CH_4 pulse was constrained in order to avoid over exposition to the reducing agent. As shown in Fig. 5B, the presence of water does not significantly modify the dynamics of the formation of the various products, since CO_2 prevails at the beginning of the CH_4 pulse whereas CO and H_2 are preferentially formed upon

increasing the catalyst degree of reduction. However in this case no significant amounts of carbonaceous deposits are formed on the catalyst surface during the CH_4 switch, as pointed out by the absence of CO_x formation during the O_2 pulse. The same behavior was observed during several repeated redox cycles.

4. Conclusions

The present investigation addressed the preparation and the redox properties of Ni–Al–O and Ni–Mg–Al–O mixed oxides as candidate materials for the chemical looping combustion process.

The results demonstrated that co-precipitation in aqueous medium using nitrates as metal precursors and $(NH_4)_2CO_3$ as precipitating agent is effective to obtain quantitative precipitation for the Ni–Al–O systems, whereas significant Mg losses occurred in the case of Ni–Mg–Al–O. Upon calcination at 1000 °C all the Ni–Al–O samples consist of two phases: cubic NiO and $NiAl_2O_4$ spinel. A similar phase composition is obtained in the Ni–Mg–Al–O, with Mg partitioned in the two phases, but mainly included in the spinel one. The presence of the spinel phase was found quite effective in preventing crystal size growth of NiO. Such an effect decreases on increasing the $NiO/NiAl_2O_4$ ratio; however the samples with the highest Ni content (i.e. 30 and 60% (w/w) NiO) still retain a crystal size which is 1/4–1/3 of the pure NiO calcined at the same temperature. Addition of Mg was found to further limit the sintering of the cubic oxide phase.

H_2-TPR experiments showed that reduction occurs in two main steps associated with NiO and $NiAl_2O_4$, respectively. Addition of Mg was found to stabilize Ni^{2+} in both the cubic oxide and the spinel phase, increasing the reduction temperature of 250 and 150 °C, respectively. Addition of Mg also markedly improves regenerability upon repeated redox cycles; no differences in the redox behavior and no changes in the crystal size were observed during five repeated H_2-TPR/TPO cycles with TPR up to 900 °C which resulted in complete reduction of Ni in the cubic oxide.

CH_4-TPR experiments showed abundant formation of coke over both Ni–Al–O and Ni–Mg–Al–O. Using the Mg-containing system, experiments at constant temperature with alternate pulses of CH_4-reducing and air-oxidizing atmosphere showed that coke formation can be avoided by co-feeding H_2O with a CH_4/H_2O molar ratio equal to 1. Also, under these conditions a good reproducibility of the redox behavior was attained. However the results of pulse experiments (and CH_4-TPR as well) clearly indicate that the Ni based systems herein investigated are poorly selective to CO_2 and H_2O being CO and H_2 by far the most abundant products of CH_4 oxidation. This is a serious limitation for the use in the CLC process where natural gas is used as fuel. Such a process requires production of CO_2 and H_2O with low CO and H_2 content from the oxidizer, in order to avoid enthalpy losses and needing for complex treatment of the exhaust gases. However the good redox stability, the possibility to avoid coke formation and the high selectivity to CO and H_2 herein demonstrated for the Ni–Mg–Al–O system could be of interest for different redox process applications, e.g. syngas production.

Acknowledgements

The financial support of SNAMPROGETTI (Italy) is acknowledged. Thanks are due to Prof. G. Artioli (Università di Milano) for helpful discussion on XRD data.

References

[1] H.J. Richter, K.F. Knocke, ACS Symp. Ser. 235 (1983) 71.
[2] M. Ishida, D. Zheng, T. Akehata, Energy Int. J. 12 (1987) 147.
[3] M. Ishida, H. Jin, Ind. Eng. Chem. Res. 35 (1996) 2469.
[4] M. Anheden, Analysis of Gas Turbine Systems for Sustainable Energy Conversion, Ph.D. Thesis, Royal Institute of Technology, Stockholm, Sweden, 2000.
[5] M. Anheden, G. Svedberg, Energy Convers. 39 (1998) 1967.
[6] J. Mc Carty, M. Gusman, D.M. Lowe, D.L. Hildebrand, K.N. Lau, Catal. Today 47 (1999) 5.
[7] J.R. Rostrup-Nielsen, T. Rostrup Nielsen, CatTech 6 (2002) 150.
[8] H. Jin, T. Okamoto, M. Ishida, Ind. Eng. Chem. Res. 38 (1999) 126.
[9] M. Ishida, M. Yamamoto, T. Ohba, Energy Convers. Manage. 43 (2002) 1469.
[10] A.C. Larson, R.B. Von Dreele, Document LAUR 86-748, Los Alamos Laboratory, 1995.
[11] H.P. Klug, L.E. Alexander, X-Ray Diffraction Procedures, Wiley, New York, 1974.
[12] L. Lietti, I. Nova, G. Ramis, L. Dall'Acqua, G. Busca, E. Giamello, P. Forzatti, F. Bregani, J. Catal. 187 (1999) 419.

[13] E.M. Levin, C.R. Robbins, H.F. McMurdie, in: M.K. Reser (Ed.), Phase Diagrams for Ceramists, The American Ceramic Society, USA, 1985, p. 2323.
[14] F. Basile, G. del Piero, F. Trifirò, A. Vaccari, J. Catal. 173 (1998) 247.
[15] C.P. Li, Y.-W. Chen, Thermochim. Acta 256 (1995) 457.
[16] K. Schultze, W. Makowsky, R. Chyzy, R. Dziembaj, G. Geisman, Appl. Clay Sci. 18 (2001) 59.
[17] J.R. Rostrup Nielsen, in: J.R. Anderson, M. Boudart (Eds.), Catalysts Science and Technology, vol. 5, Springer, Berlin, 1984 (Chapter 1).